Multi-Perspective Target Classification

Michele Vespe, Chris J. Baker, Hugh D. Griffiths
Department of Electronic and Electrical Engineering
University College London
London
United Kingdom

m.vespe@ee.ucl.ac.uk

ABSTRACT

High resolution range profiling and imaging have been the principal methods by which more and more detailed target information can be collected by radar systems. The level of detail that can be established may then be used to attempt classification. However, this has typically been achieved using monostatic radar viewing targets from a single perspective. In this paper, a multi-perspective approach to radar target classification is presented. Two datasets have been used to test the potential of multiple signatures on the mitigation of those factors leading to misclassification. The effect on the classification capability of the angular displacement between the perspectives is analysed using 1-D signatures from ADAS data, highlighting how the observed features relate to the structures that compose the target. The classification performance, examined in terms of Receiver Operator Characteristic (ROC) curves is then presented using the 2-D MSTAR data for a population formed by six classes plus two unknown and two independent targets.

1.0 INTRODUCTION

The ability to remotely classify radar targets on a day/night, all weather basis, over wide areas has long made radar a key sensor in many military and civilian applications. A number of factors leading to misclassification still make Automatic Target Recognition (ATR) an unreliable task. In order to improve the target representation, and therefore the classification performance, most of the approaches have been focusing on forming higher and higher spatial resolution [1,2], often combined to polarimetric description of the backscattering [2,3]. There has been little research published examining the effectiveness of angular diversity for improving classification performance [4]. The main concept of this research work has been inspired by human behaviour (i.e. looking form a different perspective those objects presenting ambiguous features from particular aspects) and by some echo-locating mammals using biological sonar, sometimes flying circular trajectories around the prey during the intermediate capture phase, between the detection and the final approach [5].

The M-P classification can be performed either by netted radar systems, where each node represents a perspective, or by an airborne radar flying past the target collecting multiple perspectives or by a stationary system sensing moving targets. The former application could exploit the bistatic mode of operation between the nodes, working as a Multiple-Input-Multiple-Output (MIMO) system. However, in this work, each perspective is a monostatic signature from the target.

It is worth noting that there are no rigorous and universally accepted definitions for the terms ‘classification’ and ‘recognition’. In this paper the terms are used interchangeably to address the ability of the radar system and subsequent processing to determine the class to which a target belongs.

Vespe, M.; Baker, C.J.; Griffiths, H.D. (2006) Multi-Perspective Target Classification. In *Bistatic-Multistatic Radar and Sonar Systems* (pp. 10-1 – 10-8). Meeting Proceedings RTO-MP-SET-095, Paper 10. Neuilly-sur-Seine, France: RTO. Available from: http://www.rto.nato.int/abstracts.asp.

After a brief section listing the principal reasons yielding traditional mono-perspective ATR unreliability, the Multi-Perspective (M-P) problem is introduced and its possible applications are presented. This is followed by the results of the aspect diversification effects on the Correct Classification Rates (CCRs) and their dependency on the angular displacement formed between the perspectives. The M-P classification improvement is shown and corroborated using two distinct sets of real data: the Airborne Data Acquisition System (ADAS) provided by Thales Defence and the public release Moving and Stationary Target Acquisition and Recognition (MSTAR) dataset. A final section will summarise the work reported.

2.0 FACTORS LEADING TO MISCLASSIFICATION

A number of factors responsible for the range profile variability, and as a consequence of the ATR performance deterioration are strictly aspect dependent. The *measurement noise*, caused by the thermal noise at the receiver, usually upsets the radar signatures, as well as the *Electro-Magnetic Interference* (EMI) due to other telecommunication systems in the neighbourhood of the receiver. Another source of misclassification is the intentional signal interference producing a saturation of false alarm (*jamming*) at the receiver. A confusing target response can be the consequence of *clutter* (i.e. the unwanted return of objects surrounding the region of interest) and *multi-path* (delayed returns due to multiple reflection paths). For HRR profiles, slightly different target orientations, due to rotational or translational motion of the target (assuming no range migration occurs), change the relative phase between scatterers whose returns go into the same range bin and hence cause interference resulting in fluctuations in the range profile. This is known as *speckle*. The aspect angle is also a factor in determining *shadowing phenomena*: a number of scatterers may be occluded by other parts of the target (local shadowing) or by other targets (global shadowing) and therefore not be seen by the incident waveform. As a consequence, a portion of the target is unavoidably masked and the signature further corrupted. This may be thought of as a loss of information as it can often result in significant regions of the target not contributing to the measured signature or profile.

These factors can be overcome and averaged out by using further uncorrelated signatures from the target, that is using different perspectives. The employment of multiple perspectives is a way to reduce some of these effects through the exploitation of the additional information that exhibits aspect angle dependency.

3.0 ADAS DATA AND 1-D M-P CLASSIFICATION

To examine M-P classification, High Range Resolution (HRR) profiles from turntable measurements are used as the input to the classifier. The profiles are generated from an X-band radar having an instantaneous bandwidth of 500MHz. The turntable data is first prepared by removing any stationary clutter to avoid the classifier trying to exploit this consistent information. Estimation and subtraction has been performed in the frequency domain [6].

Four ground-vehicles classified as *A*, *B*, C and *D* form the sub-population problem. Each class is described by a set of one-dimensional signatures covering 360° of turntable rotation. The transmitted waveform is a linear FM chirp and the radar returns are compressed giving 30 cm of range resolution. The depression angle of the antenna (~8°) is almost constant for the different measurements and 2" is the angular turntable rotation interval between two consecutive range profiles. Therefore, 10500 range profiles are extracted from each data file over 360°. Non-coherent averaging of signatures over three profiles has been performed in order to increase the SNR [7]. In view of the fact that the range from the target is approximately constant, no alignment is needed.

A Feed-forward Artificial Networks (FANNs) algorithm using a back-propagation learning strategy is implemented as a single M-P classifier as it was shown to have the highest accuracy and lowest computational burden. A traditional single-perspective classifier, after training with a set of templates, is

tested with profiles collected from all orientations of the target (except those of the training set). In a Two-Perspective (2-P) scenario, the parameter that distinguishes the perspective node locations is their relative angular displacement $\Delta\varphi_{1,2} = \varphi_1 - \varphi_2$. Hence, after fixing $\Delta\varphi_{1,2}$ the 2-P classifier is tested with all possible pairs of HRR profiles displaced by that angle covering all the possible orientations of the target. Having a test set consisting of N profiles, the same number of pairs can be formed to test the 2-P classifier.

Features from radar signatures have been extracted in order to reduce the intrinsic redundancy of data and simplify the model. This gives a better generalisation of the results for possible input vectors not used to train the classifier. This methodology, to certain extent, decreases the overall correct classification rate but, on the other hand, makes the representation model in the feature space less complex yielding a classification process particularly consistent with those features effectively characterising the object. After the extraction of the radar length of the target and its main peaks, Principal Component Analysis (PCA) is applied [8].

Figure 1 shows the classification performance as a function of angular separation of the two perspectives. The equivalent mono-perspective performance is shown at the 0° and 360° positions. The single target classification rates show how the global accuracy depends on the particular geometric features of the target. The drop at $\Delta\varphi_{1,2}$ =180°, as previously hypothesised, is due to the multiple axes of symmetries of the targets and it is visible for all the classes. For target *B* and *C* there is also a drop at 90° indicating a possible further degree of symmetry.

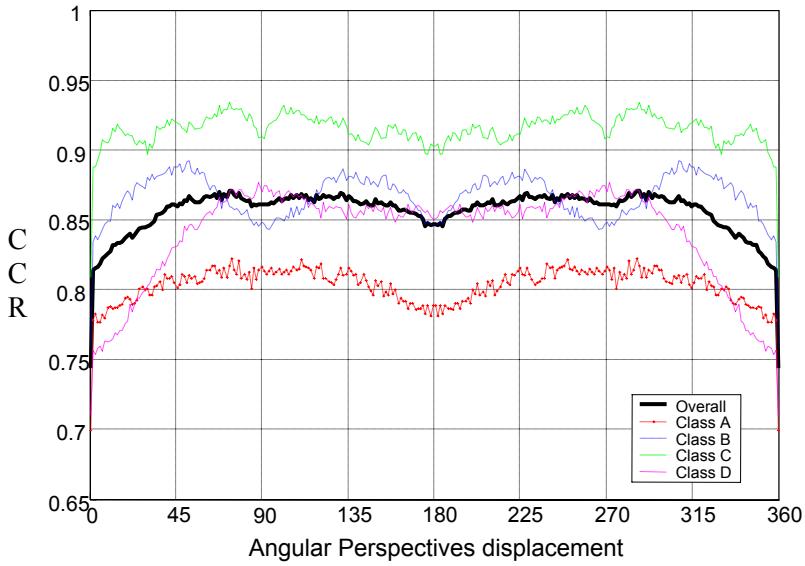

Figure 1: 2-P correct classification rates versus the angular displacement $\Delta\varphi_{1,2}$.

In Figure 2 the classification rates for three perspectives are shown. Here the first perspective is fixed whilst the other two slide around the target covering all 360°. These are shown as a function of the angular displacement $\Delta\varphi_{1,2}$ between the second and the first node, and $\Delta\varphi_{1,3}$ between the third and the first node. The origin represents the mono-perspective case and again indicates the overall improvement offered by the M-P approach. The bisector line corresponds to two radar systems at the same location, while the lines parallel to the bisector symbolise two perspectives displaced by 90° and 180°. The inherent symmetry in the radar signature of the vehicle gives rise to the relatively regular structure shown in figure 2. In a 2-P scenario, if the two nodes sense the target from the same perspective (i.e. the two radars have the same LOS) then this gives the mono-perspective classification performances. This is not the case for a 3-P network, because of weighting twice the perspective of two nodes and once the third node perspective.

As a result, the 3-P performance when $\Delta\varphi_{1,2} = 0$ and $\Delta\varphi_{1,3} \neq 0$ is worse than the 2-P scenario that simply neglects one of the coinciding perspectives. The nodes location corresponding to the higher classification performances are now different from the 2-P case: they appear for the nodes covering an aperture of 120° and equally spaced by 60°, that is configuration "a". "b" and "d" and so forth. Correct classification rates are also maximised when the nodes are equally displaced by 120° (topology "c"). Nevertheless, the difference between the maximum and average classification rates is about 1%. As has been observed for the 2-P case, the classification performance is less sensitive to the aspect angle when considering a greater number of target classes. This may suggest that in a real environment with a large number of classes, the M-P classification could be equally effective for any target position provided that each node's LOS is spaced enough from the others in order to collect uncorrelated signatures.

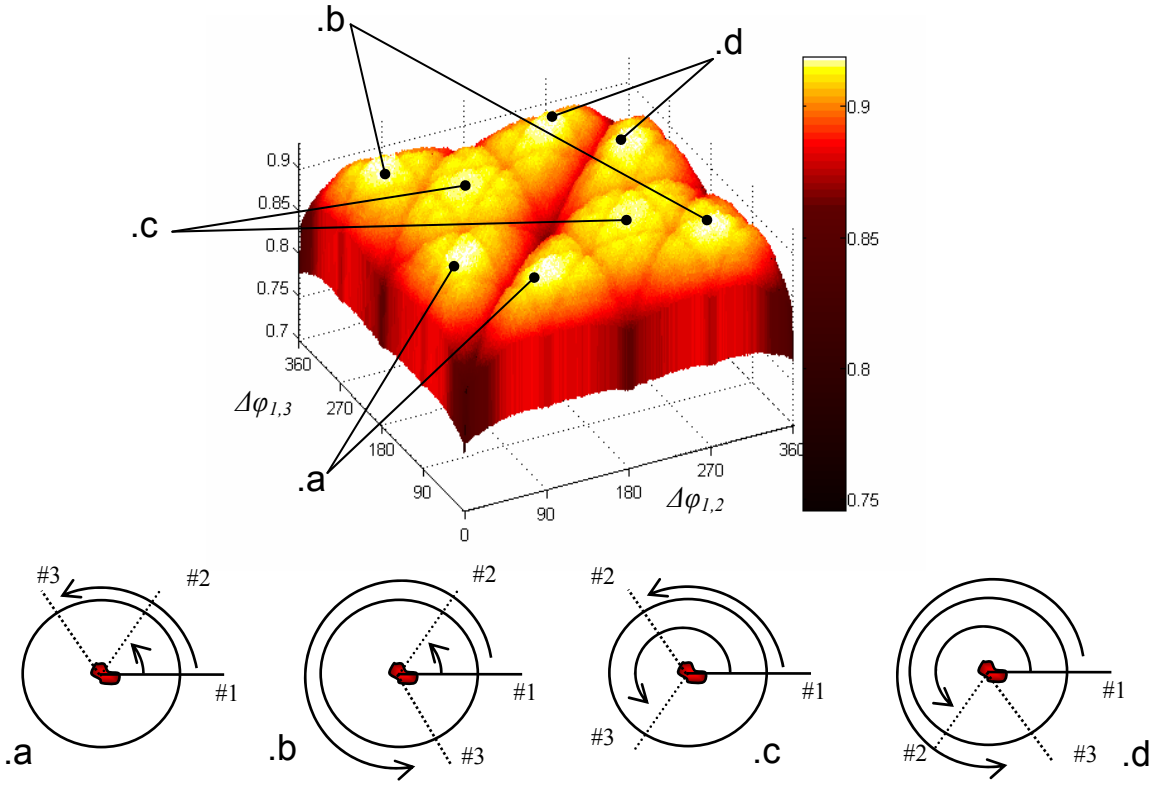

Figure 2: 3-P correct classification rates versus the angular displacements: $\Delta\varphi_{1,2}$ and $\Delta\varphi_{1,3}$.

4.0 MSTAR DATA AND 2-D M-P CLASSIFICATION

The population of targets consists of ten military ground vehicles from MSTAR database [9] as shown in Figure 3. The images are formed in a spotlight mode covering 360º, and the resolution is approximately 30 cm in both slant and cross range. A set of SAR images collected at 17º depression is used to train the classifier, while the testing set is formed by images at 15º depression. Although the scattering centres migration becomes pronounced for 2º difference in grazing angle, classification can be successfully attempted, simulating a real world scenario where usually the templates database does not fully describe all the possible azimuth and elevation deviations relative to the target.

Six targets are selected to form the set of training classes (*T72*, *BTR70*, *BMP2*, *C2S1*, *T62*, and *ZIL131*). Two independent test targets (*T72ind* and *BMP2ind*) measure the classification performance in case of targets presenting different features from the ones used to represent the class they belong to: the

independent test target has a representation class in the template set but has not been used to train the classifier. Finally, two unknown classes (*BTR60* and *D7*) give a gauge of the classification rates in case of objects not represented in the database of the classifier (Figure 3).

Figure 3: MSTAR population set.

The need of discriminating the target radar backscattering in SAR images from the clutter return has been exhaustively treated especially in case of data-sets presenting the same target location in both the training and testing sets, that means also the same clutter conformation [10]. For this reason, the feature vector is formed after clutter cancellation. Subsequently, the information processed to form the feature vector is extracted from the images after isolating the target area and its shadow using an adaptive procedure that applies two distinct thresholds to the image on the basis of the clutter statistical parameters. Eventually, as described in the previous section, PCA is applied to reduce the dimension of the classification problem. The classification approach chosen is using Radial Basis Function Neural Networks (RBFNNs) because of their flexibility and velocity of both learning and execution phases. In this paper a Gaussian RBF has been used. Each RBF is centred on a small cluster that represents a subclass.

	T72	*BTR70*	*BMP2*	*2S1*	*T62*	*ZIL131*	*"?"*
T72	**94.9**	0.5	2.0	0.5	2.0	-	-
T72ind	**71.3**	2.6	8.7	2.6	14.9	-	-
BTR70	0.5	**98.5**	-	0.5	0.5	-	-
BMP2	3.6	1.5	**93.3**	1.0	-	0.5	-
BMP2ind	14.8	10.2	**64.8**	4.1	5.6	0.5	-
2S1	3.3	9.5	1.5	**80.3**	5.1	0.4	-
T62	5.9	0.7	4.4	1.5	**87.2**	0.4	-
ZIL131	-	-	3.7	1.1	-	**95.3**	-
BTR60(un)	-	0.4	11.3	20.8	31.0	36.5	-
D7(un)	6.3	49.6	33.2	4.3	1.2	5.5	-

Table 1: Forced decision confusion matrix

In Table I, the results of the forced decision environment (i.e. the classifier must declare a target class for any input presented so that both probability of false alarm and declaration are 100%), the correct classification rates of the RBFNNs classifier are shown for each target. Since the classifier is forced to declare, the "Unknown" column is empty. The probability of correct classification achieved is P_{cc} = 93.6% and is a measure of the classifier capability of recognising objects it was trained with. As can be observed, the classification performance on the independent targets is well below the classification rates of the relative targets used to identify a class. This is mainly due to different features exhibited by the independent targets such as different loads or turret position. This aspect makes the classification task still unreliable in many applications.

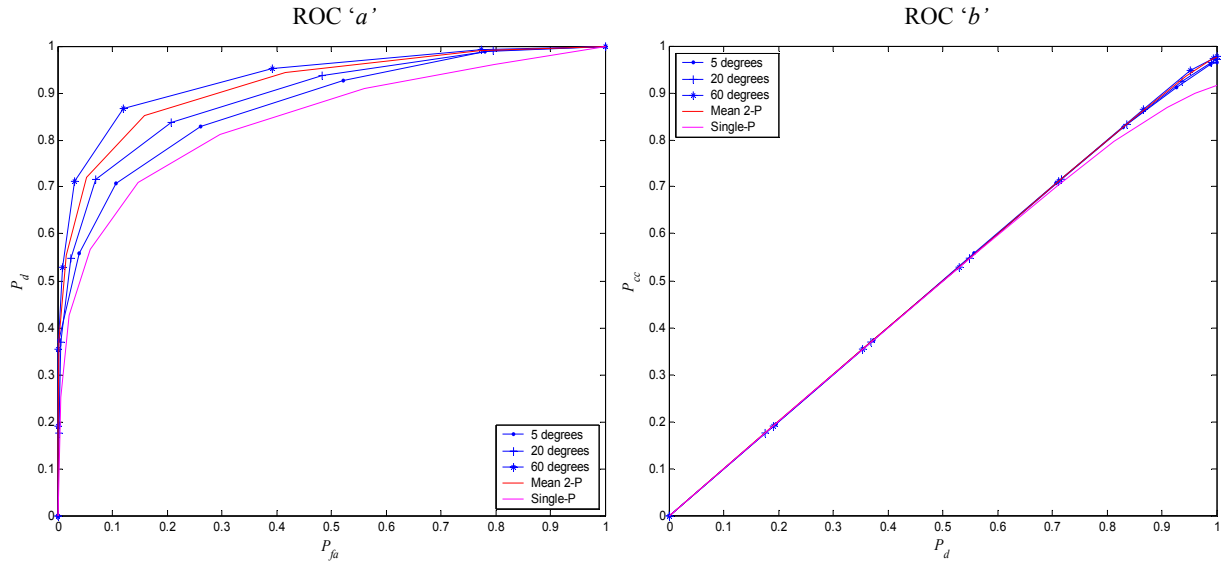

Figure 4: ROC curves.

In Figure 4, the Receiver Operator Characteristic (ROC) curves are shown: the mean value (red) of all the possible angular displacements between two radar locations over 360 degrees, the single-perspective case (magenta) and other perspective locations performances (5º, 20º, 50º and 90º). The first curve (ROC '*a*') describes the relation between probability of false alarm (P_{fa}) and probability of declaration (P_d). The probability of false alarm is proportional to the number of decisions for the unknown targets, whilst the latter is the probability of making a declaration, either correct or incorrect. The ROC '*b*' curve represents the reliability of the classifier declarations. The ideal case for the ROC 'a' is a point (P_{fa} = 0; P_d = 1), whereas in the classifier should declare only for the correct class (P_d = P_{cc}), that is represented by a straight line in the ROC '*b*' curve. The area under the curve of both curves is a measure of the reliability of the classifier. The benefits given by a second perspective are significant as the angular displacement between aspects becomes greater than the decorrelation interval required (~5º for this particular dataset). Furthermore, the mean value of the ROC curves shows the improvements over the mono-perspective case for any possible network topology (i.e. set of perspectives).

In Figure 5, the classifier probability of not declaring unknown targets (1-P_{fa}) is plotted versus the angular displacement between two perspectives. This probability is a measure of the percentage of classifying as "unknown" a target for a fixed rejection threshold. The mono-perspective classifier, for this particular example, is set to allow a probability of false alarm of 55%. As a consequence, 45% is the percentage of correct "Unknown" response. Moreover, P_{fa} fluctuates depending on the aperture between perspectives. As soon that the two perspectives decorrelate, the false alarm rate decreases and the classifier improves the ability of not declaring the targets. When $\Delta\varphi_{1,2}$ = 75º, the classifier shows a false alarm rate reduction of

almost 20% for the particular set of target used to represent the unknown class. The average improvement of the classifier capability to not declare a target (i.e. to label the input as "Unknown") is about 14% when a perspective displacement within decorrelation angular interval ($5^o < \Delta\varphi_{1,2} < 355^o$) is synthesised.

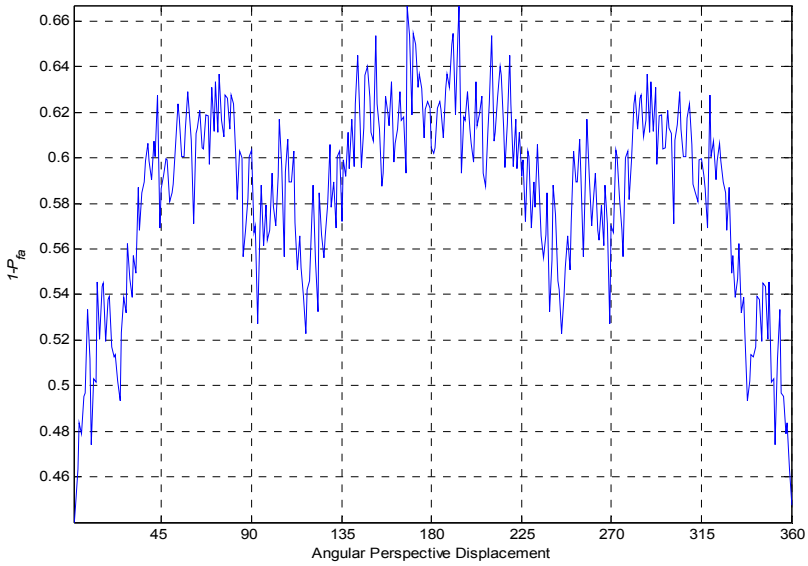

Figure 5: 2-P probability of not declaring unknown targets (1-P_{fa}).

5.0 CONCLUSIONS

In this paper, the benefits of employing multiple perspectives are examined in terms of classification rates. Clear recognition improvements are achievable for any perspective displacement between different looks, although reduced when the perspectives are closely separated because of their significant degree of correlation. However, there is a small variation in the correct classification rate for a relatively constrained set of node locations. This is due to inherent geometrical symmetries of man-made objects. The multiple perspectives affect the single class probability of correct classification differently depending mainly on the number, nature and persistency of scattering centres.

The results of employing multiple signatures sensing a radar target have been also presented using 2-D imageries of a six-class population set. The ROC curves have been described, showing the significant benefits offered by multiple perspectives. Furthermore the perspective diversification effectiveness on the relationship between false alarm rate and probability of declaration requires a greater perspective separation if compared to the one between declaration and correct classification.

6.0 ACKNOWLEDMENTS

The work reported in this paper was funded by the Electro-Magnetic Remote Sensing (EMRS) Defence Technology Centre, established by the UK Ministry of Defence and run by a consortium of Selex, Thales Defence, Roke Manor Research and Filtronic. The authors would also like to thank Thales Sensors for providing ADAS files to investigate HRR range profiles and ISAR images from real targets.

7.0 REFERENCES

[1] Rong Hu; Zhaoda Zhu: 'Researches on radar target classification based on high resolution range profiles', IEEE Aerospace and Electronics Conference, Vol. 2, July 1997, pp: 951-955.

[2] Novak, L. M.; Halversen, S. D.; Owirka, G.; Hiett, M.: 'Effects of polarization and resolution on SAR ATR', IEEE Transactions on Aerospace and Electronic Systems Vol. 33, Issue 1, Jan. 1997, pp: 102-116.

[3] Sadjadi, F.: 'Improved target classification using optimum polarimetric SAR signatures', IEEE Transactions on Aerospace and Electronic Systems Vol. 38, Issue 1, Jan. 2002 pp: 38-49.

[4] Shihao Ji; Xuejun Liao; Carin, L.: 'Adaptive multiaspect target classification and detection with hidden Markov models', IEEE Sensors Journal, Vol. 5, Issue 5, Oct. 2005, pp: 1035-1042.

[5] University of Maryland, Auditory Neuroethology Laboratory: www.bsos.umd.edu/psyc/batlab/

[6] G. A. Showman, M. A. Richards, K. J. Sangston: 'Comparison of two algorithms for correcting zero-Doppler clutter in turntable ISAR imagery', Asilomar Conference on Signals, Systems & Computers, 1, pp 411- 415, 1998.

[7] M. I. Skolnik: Introduction to Radar Systems, McGraw Hill, 1980.

[8] C. M. Bishop: Neural Networks for Pattern Recognition, Oxford University Press, Oxford, 1995.

[9] Air Force Research Laboratory: www.sdms.afrl.af.mil/datasets/mstar

[10] R. Schumacher, J. Schiller, 'Non-cooperative target identification of battlefield targets-classification results based on SAR images', 2005 IEEE International Radar Conference, pp. 167-172.